First Exclusive Measurement of Deep Virtual Compton Scattering off ^{4}He: Toward the 3D tomography of nuclei

M. Hattaway,[1,2] N.A. Baltzell,[1,3] R. Dupré,[1,2,*] K. Hafidi,[1] S. Stepanyan,[3] S. Bultmann,[4] R. De Vita,[5] A. El Alaoui,[1,6] L. El Fassi,[7] H. Egiyan,[3] F.X. Girod,[3] D. Jenkins,[8] S. Liuti,[9] Y. Perrin,[2] B. Torayev,[4] and E. Voutier[2]

(The CLAS Collaboration)

[1]*Argonne National Laboratory, Argonne, Illinois 60439*
[2]*Institut de Physique Nucléaire, CNRS/IN2P3 and Université Paris Sud, Orsay, France*
[3]*Thomas Jefferson National Accelerator Facility, Newport News, Virginia 23606*
[4]*Old Dominion University, Norfolk, Virginia 23529*
[5]*INFN, Sezione di Genova, 16146 Genova, Italy*
[6]*Universidad Técnica Federico Santa María, Casilla 110-V Valparaíso, Chile*
[7]*Mississippi State University, Mississippi State, MS 39762-5167*
[8]*Virginia Polytechnic Institute and State University, Blacksburg, Virginia, 24061*
[9]*University of Virginia, Charlottesville, Virginia 22901*

(Dated: February 20, 2017)

We report the first fully exclusive measurement of coherent Deeply Virtual Compton Scattering off a nucleus for $A > 1$. The experiment used the 6 GeV electron beam from the CEBAF machine at Jefferson Lab incident on a ^{4}He gas target in the center of the CEBAF Large Acceptance Spectrometer. A new Radial Time Projection Chamber was used to detect the recoiling ^{4}He nuclei and ensure the exclusivity of the process. The measured Beam Spin Asymmetries are larger than that observed on the proton in the same kinematic domain. Since ^{4}He is a spin zero target, we were able to extract, in a completely model independent way, the real and imaginary parts of the ^{4}He Compton Form Factors, $\mathcal{H}_A$, which are functions of the Generalized Parton Distribution H_A. This pioneering measurement of coherent Deeply Virtual Compton Scattering on the ^{4}He nucleus, with a fully exclusive final state via nuclear recoil tagging, leads the way toward 3D imaging of the partonic structure of nuclei.

PACS numbers: Valid PACS appear here

Rich information on Quantum Chromodynamics (QCD) can be extracted from the internal structure of hadrons. In the recent past, development of the Generalized Parton Distributions (GPDs) framework has offered a possibility to obtain new information about the momentum and spatial degrees of freedom of the quarks and gluons inside hadrons [1–5]. In impact parameter space, the GPDs are indeed interpreted as a tomography of the transverse plane for partons carrying a certain longitudinal momentum [6–9].

The most promising way to access GPDs experimentally is through the measurement of Deep Virtual Compton Scattering (DVCS), i.e. the hard exclusive electroproduction of a real photon. While other processes are known to be sensitive to GPDs, the measurement of DVCS is considered the cleanest probe and has been the focus of worldwide efforts [10–21] involving several accelerator facilities such as Jefferson Lab (JLab), HERA and CERN. The vast majority of these measurements focused on the study of proton structure and allowed extraction of the tomography of the nucleon (for details on the formalism, see [22–27]). This framework is also applicable to nuclei, giving access to completely new information about nuclear structure in terms of quarks and gluons [28]. Study of the 3D structure of nuclei appears to be especially important in light of the large nuclear effects observed in nuclear parton distribution functions [29–31].

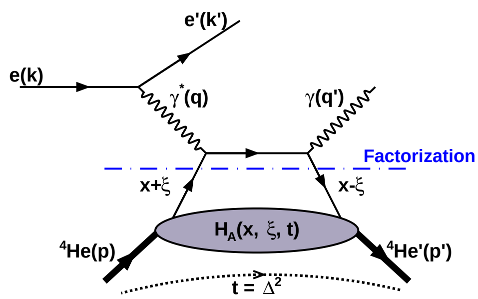

FIG. 1: Representation of the leading order handbag diagram of the DVCS process off ^{4}He.

One must overcome two major experimental challenges in measuring coherent nuclear DVCS, $eA \to' A'\gamma$. First, the cross section of coherent scattering is suppressed due to the nuclear form factor, and second, the recoil nucleus (A') must be detected to ensure coherence. Figure 1 illustrates the hand bag diagram for coherent DVCS on ^{4}He. Similar to the proton case, at large virtual photon's 4-momentum square $Q^2 = -(k-k')^2$ and small squared momentum transfer $t = (p-p')^2$ (in terms of the electron, $k(k')$, and ^{4}He, $p(p')$, four-vectors), the DVCS handbag diagram can be factorized into two parts [32, 33]. The hard part includes the photon-quark interaction and is

*corresponding author: dupre@ipno.in2p3.fr

calculable in perturbative QCD. The non-perturbative part is parametrized in terms of GPDs, which embed the partonic structure of the hadron. The GPDs depend on the three variables x, ξ and t as introduced in Figure 1. The parameter ξ relates to the Bjorken variable x_B: $\xi \approx \frac{x_B}{2-x_B}$, where $x_B = \frac{Q^2}{2M\nu}$ with M the proton mass and $\nu = k^0 - k^{0\prime}$, the t is squared momentum transfer to the target. The parameter x is the quark's internal loop momentum fraction and cannot be accessed experimentally. In the experiment we measure Compton Form Factors (CFF) [27], complex amplitudes defined as:

$$\Re e(\mathcal{H}_A) = \mathcal{P}\int_0^1 dx[H_A(x,\xi,t) - H_A(-x,\xi,t)]\, C^+(x,\xi), \tag{1}$$

$$\Im m(\mathcal{H}_A) = H_A(\xi,\xi,t) - H_A(-\xi,\xi,t), \tag{2}$$

with H_A the GPD, $\mathcal{P}$ the Cauchy principal value integral, and $C^+(x,\xi)$ a coefficient function $(= \frac{1}{x-\xi} + \frac{1}{x+\xi})$.

Until now, the only available data on nuclear DVCS was from the HERMES experiment [34], where coherence in the reaction was based only on kinematic cuts on the measured scattered electron and real photon. That measurement was performed on a large set of nuclei (^{4}He, N, Ne, Kr and Xe), but the mixing of the coherent and incoherent processes could affect the measurement significantly [35]. In this regard, direct detection of the low-energy recoil nucleus is the best way to guarantee the nucleus remains intact and that the reaction did not occur on a bound nucleon. The CEBAF Large Acceptance Spectrometer (CLAS) in Hall-B at JLab is already optimized for DVCS measurements [16, 18–21].

In order to measure DVCS on ^{4}He with a fully exclusive final state, we built a specialized radial time projection chamber (RTPC) for detection and identification of low energy recoiling light nuclei. The ^{4}He nucleus is an ideal experimental target in this regard, as it is light enough to be detected in such a setting, while it is subject to significant nuclear effects [36] and has rather high density. A helium target leads to another important advantage, as the number of GPDs defined for a hadron depends on its spin. The structure of a spin zero nucleus, such as ^{4}He, is parametrized by only one chiral even GPD ($H_A(x,\xi,t)$) at leading twist, while 4 GPDs arise in the nucleon case. This significantly simplifies the interpretation of the data and allows a model independent extraction of the ^{4}He CFF ($\mathcal{H}_A$) presented at the end of this letter.

The experiment E08-024 took place in Hall-B at Jefferson Lab in 2009 using the nearly 100% duty factor, longitudinally polarized electron beam (83% polarization) at energy of 6.064 GeV. The data were collected over 40 days using a 6 atm gaseous ^{4}He target placed 64 cm upstream of the nominal center of CLAS. For DVCS experiments, the CLAS baseline design [37] is supplemented with an inner calorimeter (IC) and a solenoid. The IC extends the photon detection acceptance of CLAS to polar angles as low as 4°. The low-energy Møller electrons produced in the target form a very high rate background that is suppressed by a 5 Tesla solenoid placed around the target.

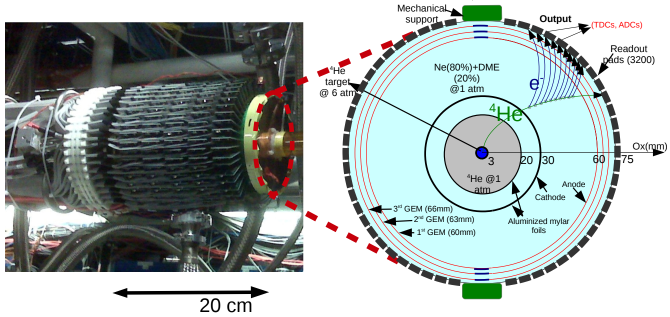

FIG. 2: Left: A picture of the E08-024 RTPC before insertion into the solenoid. Right: A cross section of the E08-024 RTPC perpendicular to the beam direction. An illustration of a ^{4}He track originating from the pressurized straw target is shown along with the electrons produced in the drift region.

In our kinematics, the recoil ^{4}He nuclei produced in DVCS have a low average momentum around 300 MeV/c. CLAS cannot detect such low energy α particles, so in order to ensure the exclusivity of the measurement, we built a small and light RTPC to complement CLAS. In Figure 2 a picture of RTPC installed in the experimental hall, and the rendering showing detector components and the ^{4}He detection concept are presented. The ^{4}He gaseous target, a 25 cm long Kapton straw with 27 μm thick wall, was part of the RTPC assembly and installed on the axis of the detector. The RTPC was calibrated specifically for the detection of ^{4}He nuclei using elastic scattering with a 1.2 GeV electron beam.

To identify coherent DVCS events, we first select events where one electron, one ^{4}He, and at least one photon are detected in the final state. Electrons are identified using measured momentum, time, and energy in the fiducial volume of the CLAS system's drift chambers, Cerenkov counters, scintillator counters, and electromagnetic calorimeters. The recoiling ^{4}He nuclei are identified in the RTPC using time, track quality, and energy loss cuts for tracks in the fiducial region. In addition, we apply a vertex matching cut to ensure that the electron and helium nucleus originate from the same position. The photons are detected in either the IC or the CLAS electromagnetic calorimeter. Note that even though the DVCS reaction has only one real photon in the final state, events with more than one good photon are not discarded at this stage. This is motivated by the fact that, while soft photons are likely to be produced in random coincidence, they cannot be mistaken for the large energy DVCS photons (> 2 GeV). The most ener-

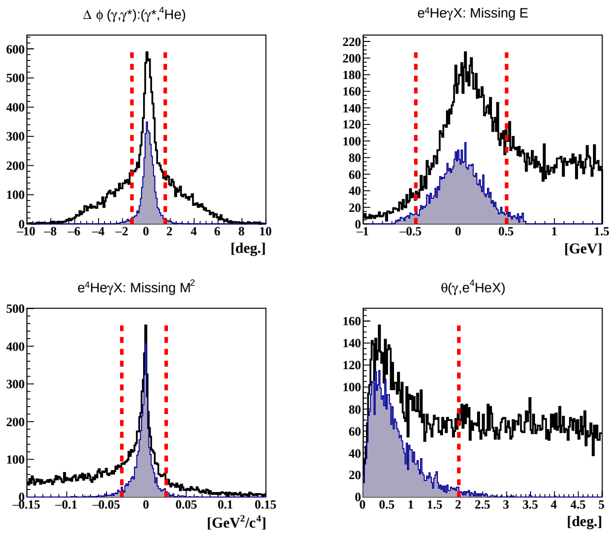

FIG. 3: Four of the six coherent DVCS exclusivity cuts. The black distributions represent the coherent DVCS events candidate. The shaded distributions represent the events which passed all the exclusivity cuts except the quantity plotted. The vertical red lines represent the applied exclusivity cuts. The distributions from left to right and from top to bottoms are: $\Delta\phi$, missing energy, missing mass squared and the cone angle (θ) between the measured and the calculated photons.

getic photon is always considered as the DVCS photon candidate.

To ensure the interaction occurs at the partonic level and the DVCS handbag diagram is dominant, we select events with $Q^2 > 1$ $[GeV^2/c^2]$. Exclusivity of the coherent DVCS reaction is optimized by applying a set of cuts on the following kinematic variables: the coplanarity angle ($\Delta\phi$), *i.e.*, the angle between the (γ,γ^*) and $(\gamma^*,^4He')$ planes, the missing energy, the missing mass squared, the missing transverse momentum of the $e'^4He'\gamma$ system, the missing mass squared of the e'^4He' system, and the angle (θ) between the measured photon and the missing momentum of the e'^4He' system. The most relevant of these cuts are presented in Figure 3, which shows 3σ cuts except for the missing energy (which appears to be too large and for which we reduced the cut window to [-0.45,0.5] GeV). We also reject events where a π^0 is identified by invariant mass reconstruction of two photons. After these requirements, we have about 3200 DVCS events left, and Figure 4 presents their kinematic distributions in (Q^2,x_B) and (Q^2,$-t$).

In this work, the physics observable extracted using coherent DVCS events is the Beam Spin Asymmetry (BSA). The BSA on an unpolarized target, A_{LU}, is measured as the difference of cross sections of the reaction at opposite beam helicities normalized to the total cross section:

$$A_{LU} = \frac{d^5\sigma^+ - d^5\sigma^-}{d^5\sigma^+ + d^5\sigma^-}, \tag{3}$$

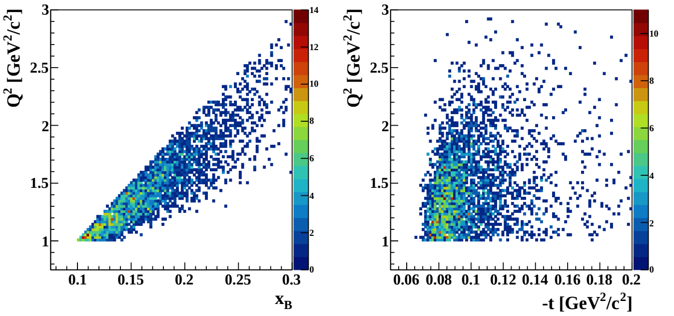

FIG. 4: Coherent DVCS event distributions for Q^2 as a function of x_B (left) and Q^2 as a function of $-t$ (right) after the exclusivity cuts.

where $d^5\sigma^{+(-)}$ is the DVCS differential cross section for a positive (negative) beam helicity. In this ratio, luminosity normalization and detector efficiencies largely cancel and A_{LU} can be expressed in terms of helicity-state yields ($N^{+/-}$)

$$A_{LU} = \frac{1}{P_B}\frac{N^+ - N^-}{N^+ + N^-}, \tag{4}$$

where P_B is the beam polarization.

The DVCS and well-known Bethe-Heitler (BH) processes, where the real photon is emitted by the incoming or the outgoing lepton, have the same final state and are indistinguishable. The amplitude of real photon electroproduction is a sum of the amplitudes of these two processes. The BH amplitude is defined by the target form factors, while the DVCS amplitude is a combination of the form factors and GPDs. At our kinematics, the cross section of real photon electroproduction is dominated by the BH contribution, while the DVCS contribution is very small. Its effect is however enhanced in the observables sensitive to the interference term, *e.g.* beam spin asymmetry. The three terms entering the cross section calculation, the BH and DVCS amplitudes squared and their interference term, can be decomposed into a finite sum of Fourier harmonics in the azimuthal angle ϕ between the (e,e') and $(\gamma^*,^4\mathrm{He}')$ planes, as shown for the nucleon in [38] and for the spin-zero targets in [39, 40]. Based on this work, the beam-spin asymmetry (A_{LU}) of a spin-zero hadron can be expressed as:

$$A_{LU}(\phi) = \frac{\alpha_0(\phi)\,\Im m(\mathcal{H}_A)}{\alpha_1(\phi) + \alpha_2(\phi)\,\Re e(\mathcal{H}_A) + \alpha_3(\phi)\left(\Re e(\mathcal{H}_A)^2 + \Im m(\mathcal{H}_A)^2\right)}, \tag{5}$$

where $\Im m(\mathcal{H}_A)$ and $\Re e(\mathcal{H}_A)$ are the imaginary and real parts of the ^{4}He CFF $\mathcal{H}_A$ that depends on the GPD H_A. In Eq. 5, ϕ is the azimuthal angle between the (e,e') and $(\gamma^*,^4\mathrm{He}')$ planes. The kinematic factors α_i depend on azimuthal angle ϕ, the nuclear form factor $F_A(t)$, Q^2 and x_B. These factors are written as:

$$\alpha_0(\phi) = \frac{x_A(1+\epsilon^2)^2}{y} S_{++}(1)\sin(\phi), \quad (6)$$

$$\alpha_1(\phi) = c_0^{BH} + c_1^{BH}\cos(\phi) + c_2^{BH}\cos(2\phi), \quad (7)$$

$$\alpha_2(\phi) = \frac{x_A(1+\epsilon^2)^2}{y}\left(C_{++}(0) + C_{++}(1)cos(\phi)\right), \quad (8)$$

$$\alpha_3(\phi) = \frac{x_A^2 t(1+\epsilon^2)^2}{y}\mathcal{P}_1(\phi)\mathcal{P}_2(\phi)\cdot 2\frac{2-2y+y^2+\frac{\epsilon^2}{2}y^2}{1+\epsilon^2}, \quad (9)$$

where $x_A = \frac{x_B M_N}{M_A}$ with $M_A(M_N)$ is the ^{4}He (nucleon) mass, $\epsilon = \frac{2x_A M_A}{\sqrt{Q^2}}$ and $y = \frac{Q^2}{2x_A M_A E_{beam}}$, $\mathcal{P}_1(\phi)$ and $\mathcal{P}_2(\phi)$ are the Bethe-Heitler propagators. The factors $c_{0,1,2}^{BH}$, c_0^{DVCS}, $c_{0,1}^{INT}$ and s_1^{INT} are the Fourier coefficients of the BH, and $S_{++}(1)$, $C_{++}(0)$, and $C_{++}(1)$ are the Fourier harmonics in the leptonic tensor. The explicit expressions of these terms can be found in [40] and show that, by using the $\sin(\phi)$ and $\cos(\phi)$ contributions, it is possible to extract $\Im m(\mathcal{H}_A)$ and $\Re e(\mathcal{H}_A)$ from the beam spin asymmetry.

In this work the azimuthal dependence of the BSA, A_{LU}, has been studied for a wide range of kinematics. We identified two main backgrounds to our measurement, accidental coincidences and exclusive coherent π^0 production. The accidentals have particles originating from different events, and we estimate their contribution to be 4.1% of our sample. We evaluated this contribution by selecting events passing all our cuts but with an electron and helium originating from different vertices. Regarding the π^0 production, it can easily be mistaken for DVCS when one of the two photons from the π^0 decay is produced at low energy in the laboratory frame and remains undetected. To estimate the importance of this background, we developed an event generator tuned on the experimental yield of exclusive π^0 measured by our experiment. We used this generator together with a GEANT3 simulation of our detector to estimate the ratio between the number of π^0 events where the two photons are detected and those that is misidentified as DVCS events. This ratio is then multiplied by the measured yield of exclusive π^0 events to correct the DVCS data. Depending on the kinematics, we found contaminations of 2 to 4%. The study of systematic uncertainties showed that the main contributions come from the choice of the DVCS exclusivity cuts (8%) and the large binning size (5.1%). However, added quadratically,the total systematic uncertainty is about 10%, which is significantly smaller than statistical uncertainties in all kinematical bins.

Due to limited statistics, dependence on the kinematical variables Q^2, x_B, and t has been studied separately. In Figure 5, A_{LU} for the three sets of binning is presented. The curves on the plots are fits with the function

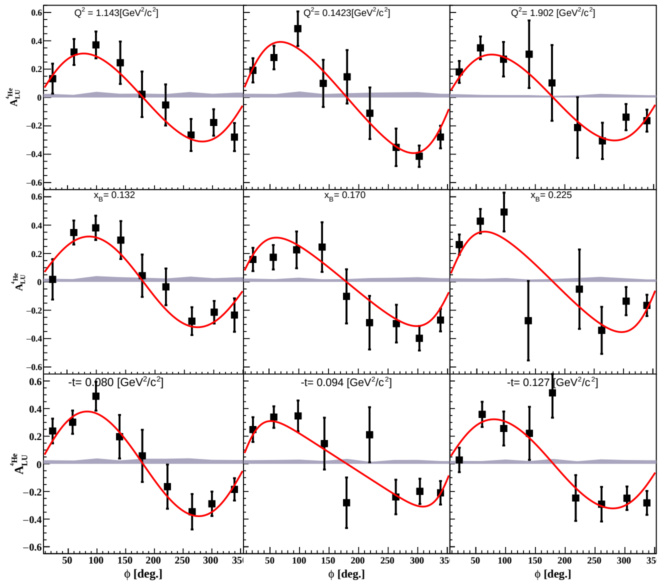

FIG. 5: The coherent A_{LU} as a function of ϕ. Results are presented for different Q^2 bins (top panel), x_B bins (middle panel), and $-t$ bins (bottom panel). The error bars represent the statistical uncertainties. The gray bands represent the systematic uncertainties, including the normalisation uncertainties. The red curves are the results of our fits with the form of equation 5.

presented in Eq. 5, where the real and imaginary parts of the CFF $\mathcal{H}_A$ are the free parameters of the fit. In Figure 6 the Q^2, x_B, and $-t$-dependencies of the fitted A_{LU} at $\phi = 90°$ are shown. The x_B and $-t$-dependencies are compared to theoretical calculations performed by S. Liuti and K. Taneja [41]. The model relies on the impulse approximation and uses advanced spectral functions of nuclei. The calculations are at slightly different kinematics than our data but still provide some guidance. The experimental results appear to have larger asymmetries than the calculations. These differences may arise from nuclear effects, such as long-rage interactions, which are not taken into account in the model.

The Q^2, X_B, and t dependencies of the ^{4}He CFF $\mathcal{H}_A$ extracted from the fit to the azimuthal dependence of A_{LU} are shown in Figure 7. Curves on the graphs are model calculations, labelled *convolution* and *off-shell*. In the convolution model [42], the nucleus is assumed to be composed of non-relativistic nucleons, each interacting independently with the probe. The Convolution-Dual model is based on nucleon GPDs from the dual parametrization [43], where the Convolution-VGG uses nucleon GPDs from the VGG model and is based on the double distributions ansatz [45]. The off-shell model [46] relies on the impulse approximation and uses advanced spectral functions of nuclei that account for all configurations of the final nuclear system and the binding effects between the nucleons.

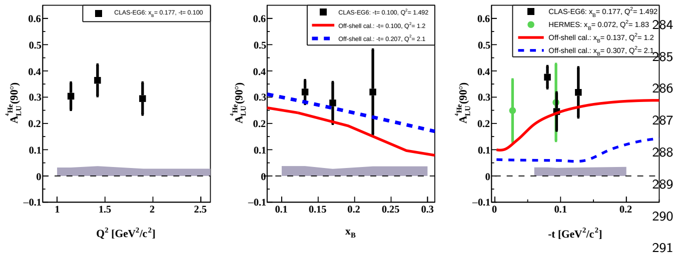

FIG. 6: The Q^2 (left), x_B (middle), and $-t$-dependencies (right) of the A_{LU} at $\phi = 90°$ (black squares). On the middle plot: the full-red and the dashed-blue curves are theoretical calculations from [41]. On the right: the green circles are the HERMES $-A_{LU}$ (positron beam was used) inclusive measurements [11], the colored curves represent theoretical calculations from [41].

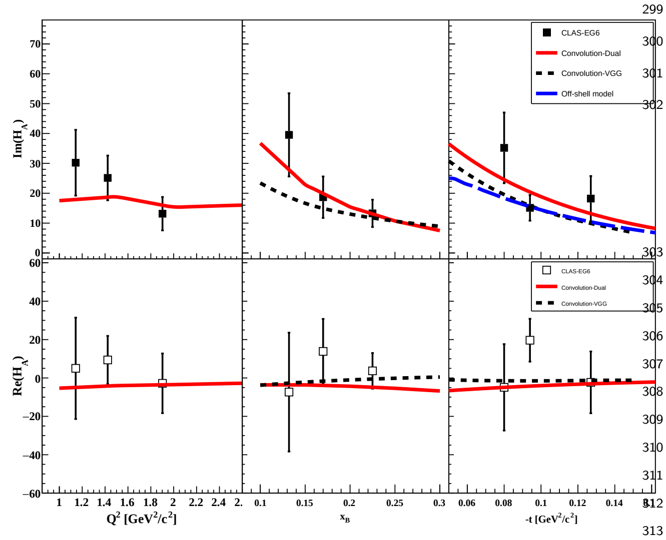

FIG. 7: The model-independent extraction of the imaginary (top panel) and real (bottom panel) parts of the ^{4}He CFF $\mathcal{H}_A$, as functions of Q^2 (right panel), x_B (middle panel), and t (left panel). The full red curves are calculations based on an on-shell model from [42]. The black-dashed curves are calculations from a convolution model based on the VGG model for the nucleons' GPDs [44]. The blue long-dashed curve on the top-right plot is from an off-shell model based on [46].

The results in Figure 7 show that the extraction of the CFF from the beam spin asymmetry is possible without any model dependent assumptions. The amplitude and the dependencies observed as a function of Q^2, x_B, and $-t$ are in agreement with the theoretical expectations. One can see a difference between the precision of the extracted imaginary and real parts, which is expected from Eq. 5 because α_2 is much smaller than α_1. While the accuracy of our results does not allow to discriminate between the models, they demonstrate possibility of extraction of the CFF of spin 0 target in a model independent way.

In summary, we present the first exclusive measurement of coherent DVCS off ^{4}He using the CLAS spectrometer supplemented with a Radial Time Projection Chamber and a high pressure gaseous target. This setup allowed detection of the low energy ^{4}He recoils in order to ensure an exclusive measurement of the coherent DVCS process. The azimuthal dependence of the measured beam spin asymmetry (A_{LU}) has been used to extract, in model independent way, the real and the imaginary parts of the ^{4}He CFF, $\mathcal{H}_A$. The extracted CFF is in agreement with predictions of the available models. This first fully exclusive experiment opens new perspectives for studying the nuclear structure with the GPD framework and paves a way for future measurements at JLAB using 12 GeV CEBAF and upgraded equipment.

We acknowledge the staff of the Accelerator and Physics Divisions at Jefferson Lab for making this experiment possible. This work is supported by the U.S. Department of Energy, Office of Science, Office of Nuclear Physics, under contract DE-AC02-06CH11357.

[1] D. Mueller, D. Robaschik, B. Geyer, F.M. Dittes and J. Horejsi, Fortsch. Phys. **42**, 101 (1994).
[2] X.D. Ji, Phys. Rev. Lett. **78**, 610 (1997).
[3] X.D. Ji, Phys. Rev. D **55**, 7114 (1997).
[4] A.V. Radyushkin, Phys. Lett. B **380**, 417 (1996).
[5] A.V. Radyushkin, Phys. Rev. D **56**, 5524 (1997).
[6] M. Burkardt, Phys. Rev. D **62**, 071503 (2000) Erratum: Phys. Rev. D **66**, 119903 (2002)
[7] M. Diehl, Eur. Phys. J. C **25**, 223 (2002) Erratum: Eur. Phys. J. C **31**, 277 (2003)
[8] A. V. Belitsky and D. Mueller, Nucl. Phys. A **711**, 118 (2002)
[9] M. Burkardt, Phys. Rev. D **72**, 094020 (2005)
[10] S. Stepanyan *et al.* [CLAS Collaboration], Phys. Rev. Lett. **87**, 182002 (2001).
[11] A. Airapetian *et al.* [HERMES Collaboration], Phys. Rev. Lett. **87**, 182001 (2001); JHEP **1207**, 032 (2012); JHEP **1006**, 019 (2010); JHEP **0806**, 066 (2008); Phys. Lett. B **704**, 15 (2011); Phys. Rev. D **75**, 011103 (2007); JHEP **0911**, 083 (2009); Phys. Rev. C **81**, 035202 (2010); JHEP **1210**, 042 (2012).
[12] S. Chekanov *et al.* [ZEUS Collaboration], Phys. Lett. B **573**, 46 (2003).
[13] A. Aktas *et al.* [H1 Collaboration], Eur. Phys. J. C **44**, 1 (2005).
[14] S. Chen *et al.* [CLAS Collaboration], Phys. Rev. Lett. **97**, 072002 (2006).
[15] C. Muñoz Camacho *et al.* [Jefferson Lab Hall A Collaboration], Phys. Rev. Lett. **97**, 262002 (2006).
[16] F.X. Girod *et al.* [CLAS Collaboration], Phys. Rev. Lett. **100**, 162002 (2008).
[17] M. Mazouz *et al.* [Jefferson Lab Hall A Collaboration], Phys. Rev. Lett. **99**, 242501 (2007)
[18] G. Gavalian *et al.* [CLAS Collaboration], Phys. Rev. C **80**, 035206 (2009).
[19] E. Seder *et al.* [CLAS Collaboration], Phys. Rev. Lett. **114**, 032001 (2015).
[20] S. Pisano *et al.* [CLAS Collaboration], Phys. Rev. D **91**,

052014 (2015).

[21] H. S. Jo *et al.* [CLAS Collaboration], Phys. Rev. Lett. **115**, no. 21, 212003 (2015)

[22] K. Goeke, M.V. Polyakov and M. Vanderhaeghen, Prog. Part. Nucl. Phys. **47**, 401 (2001).

[23] M. Diehl, Phys. Rept. **388**, 41 (2003).

[24] X.D. Ji, Ann. Rev. Nucl. Part. Sci. **54**, 413 (2004).

[25] A.V. Belitsky and A.V. Radyushkin, Phys. Rept. **418**, 1 (2005).

[26] S. Boffi and B. Pasquini, Riv. Nuovo Cim. **30**, 387 (2007).

[27] M. Guidal, H. Moutarde and M. Vanderhaeghen, Rept. Prog. Phys. **76**, 066202 (2013).

[28] R. Dupré and S. Scopetta, Eur. Phys. J. A **52**, no. 6, 159 (2016)

[29] O. Hen, G. A. Miller, E. Piasetzky and L. B. Weinstein, arXiv:1611.09748 [nucl-ex].

[30] P. R. Norton, Rept. Prog. Phys. **66**, 1253 (2003).

[31] D. F. Geesaman, K. Saito and A. W. Thomas, Ann. Rev. Nucl. Part. Sci. **45**, 337 (1995).

[32] A. Freund and J.C. Collins, Phys. Rev. D **59**, 074009 (1998)

[33] X.-D. Ji and J. Osborne, Phys. Rev. D **58**, 094018 (1998)

[34] F. Ellinghaus *et al.* [HERMES Collaboration], AIP Conf. Proc. **675**, 303 (2003)

[35] V. Guzey and M. Strikman, Phys. Rev. C **68**, 015204 (2003)

[36] J. Seely *et al.* Phys. Rev. Lett. **103**, 202301 (2009)

[37] B. A. Mecking *et al.* [CLAS Collaboration], Nucl. Instrum. Meth. A **503**, 513 (2003).

[38] A. V. Belitsky, D. Mueller and A. Kirchner, Nucl. Phys. B **629**, 323 (2002)

[39] A. Kirchner and D. Mueller, Eur. Phys. J. C **32**, 347 (2003)

[40] A. V. Belitsky and D. Mueller, Phys. Rev. D **79**, 014017 (2009)

[41] S. Liuti and K. Taneja, Phys. Rev. C **72**, 032201 (2005)

[42] Private communications with V. Guzey based on: V. Guzey, Phys. Rev. C **78**, 025211 (2008).

[43] V. Guzey and T. Teckentrup, Phys. Rev. D **74**, 054027 (2006)

[44] Private communications with M. Guidal based on: M. Guidal, M. V. Polyakov, A. V. Radyushkin and M. Vanderhaeghen, Phys. Rev. D **72**, 054013 (2005).

[45] I. V. Musatov and A. V. Radyushkin, Phys. Rev. D **61**, 074027 (2000).

[46] Private communications with S. Liuti based on: J. O. Gonzalez-Hernandez, S. Liuti, G. R. Goldstein and K. Kathuria, Phys. Rev. C **88**, no. 6, 065206, (2013).